Nodeless Variable Adaptive Finite Element Methods
for Steady-state Heat Transfer Problems

Sutthisak Phongthanapanich

Department of Mechanical Engineering Technology,

College of Industrial Technology,

King Mongkut's University of Technology

North Bangkok, Bangkok 10800, Thailand

e-mail: sutthisakp@kmutnb.ac.th

Abstract

A nodeless variable element method is combined with the flux-based formulation to analyze two-dimensional steady-state heat transfer problems. The nodeless variable element employs quadratic interpolation functions to provide higher solution accuracy without requiring additional actual nodes. The flux-based formulation is applied to reduce the complexity in deriving the finite element equations as compared to the conventional finite element method. The solution accuracy is further improved by implementing an adaptive meshing technique to generate finite element mesh that can adapt and move along with the solution behavior. The effectiveness of the combined procedure is evaluated by steady-state heat transfer problems that have exact solutions.

Keywords: Flux-based formulation, Adaptive finite element method, Heat transfer.

1. Introduction

The finite element method has been widely used to solve for the response of aerospace structures caused by the thermal effect in the past decades [1,2]. The solution accuracy is improved by simply refining the finite element model using consecutively smaller elements until a required convergence is met. The solution accuracy can also be improved by using the *h*-method of adaptation where the mesh is globally or locally refined or coarsened [2-6], or the *p*-method by increasing or decreasing the order of the element interpolation functions [7]. Recently, many researchers have proposed improved versions of the *r*-refinement method with moving mesh, so that mesh points are moved throughout the domain while the connectivity of the mesh is kept fixed [8].

The objective of this paper is to develop a procedure to improve the predicted temperature distribution [2] by using an alternative finite element method. The nodeless variable finite element is introduced and

employed in this paper in order to increase the temperature solution accuracy. The nodeless variable finite element uses quadratic interpolation functions to describe the temperature distribution over the element without requiring additional actual nodes. The paper also introduces and implements the flux-based formulation to derive the finite element matrices for such nodeless variable element. The flux-based formulation can simplify the finite element computational procedure as compared to the conventional finite element method. The effectiveness of the combined procedure is also evaluated by several steady-state heat transfer problems that have exact solutions.

2. Nodeless Finite Element Formulation

For two-dimensional domain Ω bounded by surface S in the x-y coordinate system as shown in Fig. 1, the two-dimensional steady-state energy equation can be written in the conservation form as,

$$\frac{\partial E}{\partial x} + \frac{\partial F}{\partial y} = Q(x, y) \qquad (1)$$

where $Q(x,y)$ denotes the heat source function. The flux components E and F are defined by,

$$E = -k\frac{\partial T}{\partial x} \quad \text{and} \quad F = -k\frac{\partial T}{\partial y} \qquad (2)$$

where T is the temperature and k is the thermal conductivity. The Poisson's equation shown in Eq. (1) is to be solved together with appropriate boundary conditions that may consist of,

$$T_1(x, y) \quad \text{on } S_1 \qquad (3a)$$

$$k\frac{\partial T}{\partial n} + h(T - T_\infty) = q \quad \text{on } S_2 \qquad (3b)$$

where h is convection coefficient, T_∞ is medium temperature for convection, and q is the heat flux normal to the surface boundary.
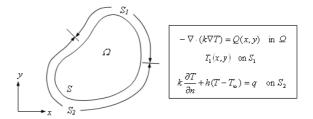

Fig. 1. Two-dimensional domain and boundary conditions for problem governed by energy equation

The flux-based formulation is used herein to derive the finite element equations associated with the nodeless variable element. For the triangular nodeless variable element, the distribution of the temperature over the element is assumed in the form,

$$T(x, y) = \sum_{i=1}^{6} N_i(x, y)T_i = \lfloor N(x, y)\rfloor\{T\} \qquad (4)$$

where $\lfloor N(x,y) \rfloor$ consists of the element interpolation functions, and $\{T\}$ is the vector of the unknown temperature variables (T_1 - T_3) and the nodeless variables (T_4 - T_6). The element interpolation functions, N_1, N_2, N_3 are identical to the element interpolation functions L_1, L_2, L_3 used for the standard three-node triangular element [5]. The nodeless variable interpolation functions implemented in this paper are,

$$N_4 = L_2 L_3 \;\; ; \;\; N_5 = L_1 L_3 \;\; ; \;\; N_6 = L_1 L_2 \quad (5)$$

To derive the finite element matrices by means of the flux-based formulation, the method of weighted residuals is first applied to Eq. (1),

$$\int_{\Omega} N_i \left(\frac{\partial E}{\partial x} + \frac{\partial F}{\partial y} - Q(x,y) \right) d\Omega = 0 \quad (6)$$

where Ω is the element domain. The Gauss's theorem is then applied to the flux derivative terms to yield,

$$\int_{\Omega} N_i \frac{\partial E}{\partial x} d\Omega = \int_{S} N_i E n_x d\Gamma - \int_{\Omega} \frac{\partial N_i}{\partial x} E d\Omega \quad (7a)$$

$$\int_{\Omega} N_i \frac{\partial F}{\partial y} d\Omega = \int_{S} N_i F n_y d\Gamma - \int_{\Omega} \frac{\partial N_i}{\partial y} F d\Omega \quad (7b)$$

where S is the element boundary. Substituting Eqs. 7(a)-(b) into Eq. (6) to yield,

$$\int_{\Omega} \frac{\partial N_i}{\partial x} E d\Omega + \int_{\Omega} \frac{\partial N_i}{\partial y} F d\Omega = \int_{S} N_i E n_x d\Gamma +$$
$$\int_{S} N_i F n_y d\Gamma - \int_{\Omega} N_i Q(x,y) d\Omega \quad (8)$$

In the flux-based formulation [2], the element flux distributions are computed from the actual nodal fluxes as,

$$E = \sum_{i=1}^{3} \overline{N}_i E_i = \lfloor \overline{N} \rfloor \{E\} \quad (9a)$$

$$F = \sum_{i=1}^{3} \overline{N}_i F_i = \lfloor \overline{N} \rfloor \{F\} \quad (9b)$$

where $\lfloor \overline{N} \rfloor$ are the standard linear element interpolation functions, i.e., $\lfloor L_1 \;\; L_2 \;\; L_3 \rfloor$. The $\{E\}$ and $\{F\}$ are the vectors of the actual nodal heat fluxes,

$$\{E\} = q_x = \left\{ \begin{array}{c} -k \left\lfloor \dfrac{\partial N}{\partial x} \right\rfloor \{T\} \Big|_1 \\[2mm] -k \left\lfloor \dfrac{\partial N}{\partial x} \right\rfloor \{T\} \Big|_2 \\[2mm] -k \left\lfloor \dfrac{\partial N}{\partial x} \right\rfloor \{T\} \Big|_3 \end{array} \right\} \quad (10a)$$

$$\{F\} = q_y = \left\{ \begin{array}{c} -k \left\lfloor \dfrac{\partial N}{\partial y} \right\rfloor \{T\} \Big|_1 \\[2mm] -k \left\lfloor \dfrac{\partial N}{\partial y} \right\rfloor \{T\} \Big|_2 \\[2mm] -k \left\lfloor \dfrac{\partial N}{\partial y} \right\rfloor \{T\} \Big|_3 \end{array} \right\} \quad (10b)$$

Substituting Eq. (10) into Eq. (8), the finite element equations are,

$$[D_x]\{E\} + [D_y]\{F\} = -\{R\} + \{B\} \qquad (11)$$

where

$$[D_x] = \int_A \left\{\frac{\partial N}{\partial x}\right\}\lfloor \overline{N} \rfloor dA \qquad (12a)$$

$$[D_y] = \int_A \left\{\frac{\partial N}{\partial y}\right\}\lfloor \overline{N} \rfloor dA \qquad (12b)$$

and A is the element area. The element nodal vector $\{R\}$ associated with the source function and the vector $\{B\}$ representing the boundary nodal flux vector are,

$$\{R\} = \int_A \{N\} Q(x,y)\, dA \qquad (13b)$$

$$\{R\} = \int_A \{N\} Q(x,y)\, dA \qquad (13b)$$

where l and m are the components of the unit vector normal to the element boundary. The vector $\{q\}$ appearing in the above Eq. (13) may be replaced by different types of boundary conditions as shown in Eq. (3b). The interpolation functions in Eq. (13) needed for integration along a typical element side s in Fig. 2 are,

$$N_1 = 1 - \frac{x}{L} \; ; \; N_2 = \frac{x}{L} \; ; \; N_3 = \frac{x}{L}\left(1 - \frac{x}{L}\right) (14)$$

where L is the length of element edge and x is the local coordinate along the edge starting from node 1. The finite element equations, Eq. (12) are derived for all the elements prior to assembling to yield the system equations. Appropriate boundary conditions of the given problem are then applied. Finally, the system equations are iteratively solved for the nodal solutions and the nodeless variables using the preconditioned conjugate gradients method with an element-by-element approximation technique [9].
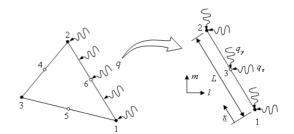

Fig. 2. Discretization of flux vector q into the actual nodes and the nodeless variable on a typical element edge.

3. Adaptive Remeshing Technique

There are two main steps in the implementation of the adaptive meshing technique, the first step is the determination of proper element sizes and the second step is the new mesh generation [2,4,5]. The temperature variable T is used as the indicator for computing proper element sizes at different locations in the domain. As small elements must be placed in the region where changes in the primary

variable gradients are large, the second derivatives of the primary variable at a point with respect to global coordinates x and y are needed. The maximum principal quantities are then used to compute the proper element size by requiring that the error should be uniform for all elements. It should also be noted that the finite element solutions are closely related to the quality of the element shapes. The mesh adaptation technique [4,5] implemented in this paper assures to provide good quality of the element shapes for all the meshes generated. According to the quality criterion presented by Ruppert [10], the minimum angle ( ) for a triangle to assure good element aspect ratio is given by,

$$\left|\frac{1}{\sin\gamma}\right| \leq \frac{d_{longest}}{d_{shortest}} \leq \left|\frac{2}{\sin\gamma}\right| \tag{14}$$

where d denotes the distance. The value of equals to 60° is used in this paper to calculate the element aspect ratio for producing the near-equilateral triangles in the process of generating all adaptive finite element meshes.

4. Algorithm Evaluation

To evaluate the performance of the nodeless variable finite element using the flux-based formulation with the implementation of the adaptive meshing technique, five boundary value problems that have exact solutions are presented. These problems consist of solving: (1) Laplace equation with Dirichlet boundary conditions, (2) Highly heat source along diagonal line, and (3) 4-steep gradient cones in a square region.

4.1 Laplace equation with Dirichlet boundary conditions

The first example for evaluating the performance of the nodeless variable flux-based finite element method is to solve the Laplace equation ($\nabla^2 U = 0$) with Dirichlet boundary conditions. The problem statement of a 1×1 square domain with the specified boundary conditions is given in Fig. 3. The exact solution for the temperature distribution is,

$$T(x, y) = x^2 + y(1 - y) \tag{15}$$

The structured finite element mesh model with 162 nodeless variable elements (100 nodes) and the predicted solution contours are shown in Fig. 4. Figure 5 shows good agreement between the exact and the predicted solutions along the edge $y = 0$.
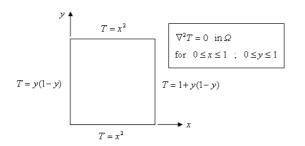
$$T(x, y) = x^2 + y(1 - y) \tag{16}$$

Fig. 3. Problem statement of the Laplace
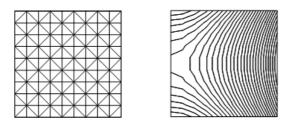equation with Dirichlet boundary conditions.

Fig. 4. Problem statement of the Laplace
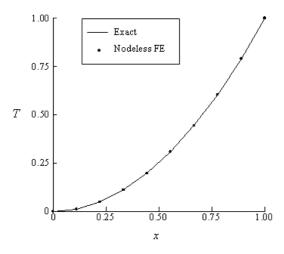equation with Dirichlet boundary conditions.

Fig. 5. Problem statement of the Laplace
equation with Dirichlet boundary conditions.

4.2 Highly heat source along diagonal line

The Poisson's equation and the boundary conditions, that produce a solution with high diagonal gradient in a square region, are shown in Fig. 6. The exact solution [2,11] as

given by Eq. (17) has been chosen to give zero values on the boundary and exhibit a sharp transition of gradients along a region near the diagonal of the domain,

$$T(x, y) = x(1 - x)y(1 - y)\tan^{-1}(100\beta) \quad (17)$$
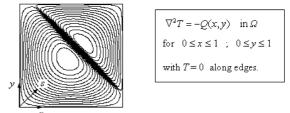
where $\beta = \sqrt{2}(x + y) - 0.8$.

Fig. 6. Governing equation, boundary conditions, and
solution contours for a highly heat source
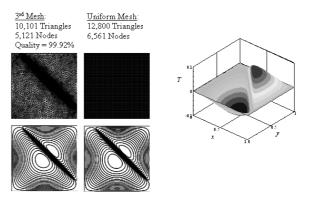along diagonal line problem.

Fig. 7. Uniform and adaptive meshes with their
solution contours for a highly heat source
along diagonal line problem.

The nodeless variable finite element solutions on adaptive meshes, and the conventional finite element solution using the standard quadratic elements on a uniformly structured mesh, are shown in Fig. 7. Figure 8

shows the comparison of the exact and the predicted solutions obtained from the nodeless variable finite element method using the adaptive meshes, and from the conventional finite element method using the standard quadratic elements on the uniformly structured mesh. The figure indicates that, in order to obtain the solution accuracy nearly at the same level as provided by the third adaptive mesh, a uniformly structured mesh (80×80 intervals) with at least 12,800 quadratic finite elements is required.
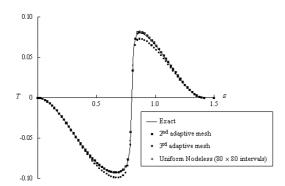

Fig. 8. Comparison of the exact and the predicted solutions for a highly heat source along diagonal line problem.

4.3 4-steep gradient cones in a square region

The governing equation and the boundary conditions, that generate a solution of the 4-steep heat gradient cones in a square region, are shown in Fig. 9. The exact solution with zero values on the boundary and exhibits 4-steep gradient cones is given by,

$$T(x,y) = \begin{cases} 0 & r > 0.075 \\ 10[1+\cos(\pi r/0.075)] & r \le 0.075 \end{cases} \quad (18)$$

The nodeless variable finite element solutions using the initial and the third adaptive meshes are shown in Fig. 10. Figure 11 shows the comparison of the exact and the predicted solutions obtained from the nodeless variable finite element method using the adaptive meshes. For this example, a uniformly structured mesh (120×120 intervals) with at least 28,800 quadratic finite elements is required in order to produce the solution accuracy nearly at the same level as provided by the third adaptive mesh.
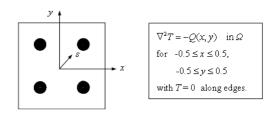

Fig. 9. Governing equation, boundary conditions, and solution contours for 4-steep gradient cones in a square region problem.

Initial Mesh:
1,648 Triangles
865 Nodes
Quality = 99.58%

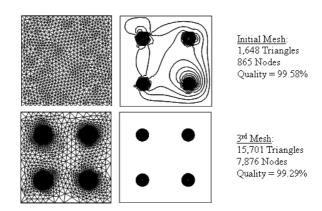3rd Mesh:
15,701 Triangles
7,876 Nodes
Quality = 99.29%

Fig. 10. Initial and adaptive meshes with their solution
contours for a 4-steep gradient cones
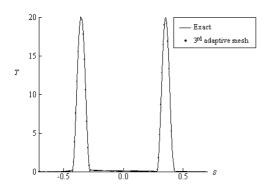in a square region problem.

Fig. 11. Comparison of the exact and the predicted
solutions for a 4-steep gradient cones in
a square region problem.

5. Conclusions

The nodeless variable flux-based finite element method was developed to solve the two-dimensional energy equation. The nodeless variable finite element and its interpolation functions were described. The flux-based formulation was developed and applied to the nodeless variable finite element for reducing the computational complexity as compared to the conventional finite element method. The solution accuracy was further improved by implementing an adaptive meshing technique. The performance of the combined procedure was evaluated by using five boundary value problems that have exact solutions. These problems demonstrate that the combined nodeless variable flux-based finite element method and the adaptive meshing technique helps increasing the analysis solution accuracy, and at the same time, reducing the total number of unknowns as compared to the standard nonadaptive finite element method.

References

[1] Noor, A.K. (1999), "Computational structures technology: Leap Frogging into the Twenty-First Century", *Comp. & Struct.*, Vol. 73, 1-31.

[2] Phongthanapanich, S. and Dechaumphai, P. (2006), "Heat Transfer Analyses by means of Flux-based Formulation and Mesh Adaptation", *Engineering Journal of SIAM University*, Vol. 12, 1-8.

[3] Wansophark, N., and Dechaumphai, P. (2006), "A Monotone Streamline Upwind Finite Element Method for 6-nodes Triangular Elements", *Engineering Journal of SIAM University*, Vol. 13, 9-16.

[4] Phongthanapanich, S., Boonmalert, P. and Dechaumphai, P. (2006), "Characteristic-based Split Finite Element Algorithm for Viscous Incompressible Flow Problems", *Engineering Journal of SIAM University*, Vol. 13, 26-31.

[5] Phongthanapanich, S. and Dechaumphai, P. (2009), "Adaptive Finite Element Method for Crack Propagation Analysis", *The Journal of KMUTNB*, Vol. 19, 154-163.

[6] Phongthanapanich, S. and Dechaumphai, P. (2004), "Mixed Entropy Fix Method for Roe's Flux-Difference Splitting Scheme with Automatic Mesh Generation", *Trans. of CSME*, Vol. 28, 531-550.

[7] Zienkiewicz, O.C. and Taylor, R.L. (2000), *Finite Element Method, volume 1: The basis*, 5th Edition, Woburn, Butterworth-Heinemann.

[8] Beckett, G., Mackenzie, J.A., and Robertson, M.L. (2001), "A Moving Mesh Finite Element Method for the Solution of Two-dimensional Stefan Problems", *J.Comput. Phys.*, Vol. 68, 500-518.

[9] Hughes, T.J.R., Levit, I., and Winget, J. (1983), "An Element-by-element solution algorithm for problems of structural and solid mechanics", *Comput. Meth. Appl. Mech. Eng.*, Vol. 36, 241-254.

[10] Ruppert, J. (1995), "A Delaunay refinement algorithm for quality 2-dimensional mesh generation", *J. Algorithm*, Vol. 18, 548-585.

[11] Dechaumphai, P. and Morgan, K. (1992), *Thermal structures and materials for High-speed flight*, AIAA, Washington, D.C..